primary importance when the number of layers is relatively small. This analysis can be easily reduced to treat plates with two distinct facings and a single core. This analysis is applicable for sandwich plates with thick or thin cores provided the facings are not so thick as to introduce appreciable transverse shear deformation in addition to that of the cores.

References

[1] Reissner, E., "Small Bending and Stretching of Sandwich-Type Shells," TN 1832, 1949, NACA.
[2] Zaid, M., "Symmetrical Bending of Circular Sandwich Plates," *Proceedings of the 2nd U.S. National Congress of Applied Mechanics*, 1954, Ann Arbor, Mich., pp. 413–421.
[3] Erickson, W. S., "Bending of Circular Sandwich Plates Under Normal Load," Rept. 1828, June 1953, U.S. Dept. of Agriculture Forest Products Lab.
[4] Kao, J. S., "Bending of Circular Sandwich Plates," *Journal of the Engineering Mechanics Division, Proceedings of the American Society of Civil Engineers*, Vol. 91, No. EM4, Paper 4449, Aug. 1965, pp. 165–176.
[5] Kao, J. S., "Circular Sandwich Plates Under Eccentric Load," *Journal of the Engineering Mechanics Division, Proceedings of the American Society of Civil Engineers*, Vol. 95, No. EM1, Feb. 1969, pp. 235–245.
[6] Stickney, G. H. and Abdulhadi, F., "Flexure Theory of Multilayer Orthotropic Circular Sandwich Plates," *Journal of Composite Materials*, Vol. 2, No. 2, April 1968, pp. 200–219.
[7] Liaw, B. D. and Little, R. W., "Bending of Multilayer Sandwich Plates," *AIAA Journal*, Vol. 5, No. 2, Feb. 1967, pp. 301–304.
[8] Kao, J. S. and Ross, R. S., "Bending of Multilayer Sandwich Beams," *AIAA Journal*, Vol. 6, No. 8, Aug. 1968, pp. 1583–1585.

Transonic Flows by Coordinate Transformation

P. O. Baronti,* S. Elzweig,† and R. Vaglio-Laurin‡
Advanced Technology Laboratories Inc.,
Jericho, N. Y.

NUMERICAL solutions of transonic flows about two dimensional airfoils have been obtained by Murman and Cole[1] by integration of the transonic small disturbance equation in a finite domain around the airfoil. The far field boundary conditions are derived analytically but they have to be periodically recalculated during the computation.

This problem is avoided if the infinite domain around the airfoil is transformed into a finite one by a transformation of the independent variables x,y to the variables suggested by Sills,[2] e.g., the variables $\xi = \tanh \alpha x$ and $\eta = 1 - e^{-\beta y}$.

In the new coordinate system, the domain being defined by $-1 \leq \xi \leq 1$ and $0 \leq \eta \leq 1$, the small disturbance equation becomes

$$\alpha^2(1-\xi^2)[(1-\xi^2)\phi_{\xi\xi} - 2\xi\phi_\xi][(1-M_\infty^2) - (\gamma+1)\alpha M_\infty^2(1-\xi^2)\phi_\xi] + \beta^2(1-\eta)[(1-\eta)\times \phi_{\eta\eta} - \phi_\eta] = 0 \quad (1)$$

and the exact boundary condition on the boundaries $\xi = \pm 1$ and $\eta = 1$ is $\phi = 0$. Along the axis, $\eta = 0$, the boundary condition is given, e.g., by $\phi_\eta = 0$, fore and aft of the airfoil, and by $\phi_\eta = F'(\xi)/\beta$ along the airfoil; $F(\xi)$ being the airfoil shape. Thus, the numerical process is reduced to seeking a relaxation solution in the finite domain, without the need of computing the far field values.

Received June 16, 1971. This work is part of an investigation supported by ONR under Contract N00014-71-C-0197.
* Senior Research Scientist. Member AIAA.
† Research Scientist.
‡ Consultant; also Professor of Aeronautics and Astronautics, New York University, New York. Associate Fellow AIAA.

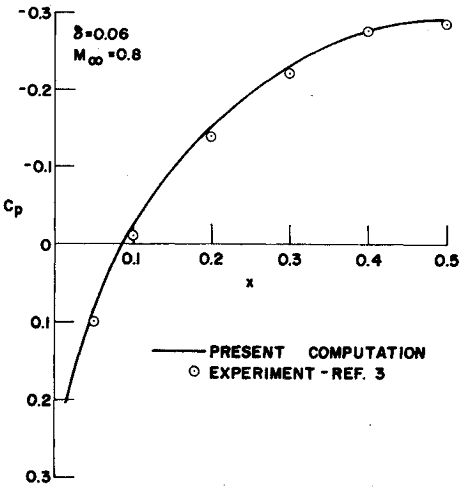

Fig. 1 Pressure coefficient along nonlifting circular arc airfoil.

A typical numerical solution of Eq. (1) for a nonlifting circular arc airfoil of thickness $\delta = 0.06$, at a freestream Mach number of 0.8, is presented here for illustrative purposes. The calculation employs a coarse mesh $\Delta\eta \simeq \Delta\xi = 0.05$ with $\alpha = \beta = 1$ and a point relaxation technique; the result is shown in Fig. 1 and compared with the experimental data of Knechtel.[3]

The computation has been repeated by using the approach of Murman and Cole. For comparable accuracy it has been found that the transformation affords considerable savings in computational time.

References

[1] Murman, E. M. and Cole, J. D., "Calculation of Plane Steady Transonic Flows," *AIAA Journal*, Vol. 9, No. 1, Jan. 1971, pp. 114–121.
[2] Sills, J. A., "Transformations for Infinite Regions and their Application to Flow Problems," *AIAA Journal*, Vol. 7, No. 1, Jan. 1969, pp. 117–123.
[3] Knechtel, E. D., "Experimental Investigation at Transonic Speeds of Pressure Distributions over Wedge and Circular Arc Airfoil Sections and Evaluation of Perforated-Wall Interference," TN D-15, 1959, NASA.

Aerodynamic Characteristics of Slender Wedge-Wings in Hypersonic Strong Interaction Flows

C. M. Rodkiewicz* and T. K. Chattopadhyay†
University of Alberta, Edmonton, Canada

THE purpose of this Note is to apply the results obtained by the present authors in Ref. 1 to predict the aerodynamic characteristics of slender two-dimensional wedge-wings in hypersonic strong interaction flow. In Ref. 1 the hypersonic strong-interaction flow over an inclined surface was analyzed using an asymptotic expansion in inverse powers of the inter-

Received June 11, 1971.
* Faculty Adviser, Department of Mechanical Engineering.
† Graduate Student, Department of Mechanical Engineering.

Fig. 1 Forces acting on a wedge-wing.

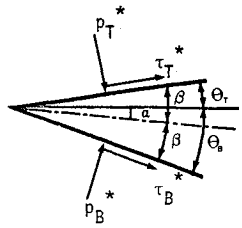

action parameter $\bar{\chi}$. Starting with an expansion of the form

$$\frac{p^*(x)}{p_\infty^*} = p_0\bar{\chi}\left[1+\frac{p_1K_b}{\bar{\chi}^{1/2}}+\frac{p_2+p_3K_b^2}{\bar{\chi}}+0(\bar{\chi}^{-3/2})\right] \quad (1)‡$$

for the pressure and similar expansions for the displacement thickness δ^*, the transformed stream function f and the nondimensional total enthalpy H, a set of four coupled simultaneous ordinary differential equations were obtained. These equations were solved numerically and the unknown constants p_0,p_1,p_2,p_3 were determined from these solutions after some algebraic manipulation.

The shear stress on the wall τ_w^* can be obtained in the form:

$$\frac{\tau_w^*}{\rho_\infty^* u_\infty^{*2}} = \frac{\bar{\chi}^{3/2}}{M_\infty^3}\tau_0\left[1+\frac{\tau_1K_b}{\bar{\chi}^{1/2}}+\frac{\tau_2+\tau_3K_b^2}{\bar{\chi}}\right] \quad (2)$$

where the constants $\tau_i(i = 0,1,2,3)$ are given by

$$\tau_0 = [(p_0)^{1/2}/2]f_0''(0) \quad (3a)$$

$$\tau_1 = p_1[1+\bar{f}_1''(0)/f_0''(0)] \quad (3b)$$

$$\tau_2 = p_2[1+\bar{f}_2''(0)/f_0''(0)] \quad (3c)$$

$$\tau_3 = p_3[1+\bar{f}_2''(0)/f_0''(0)] + p_1^2[(\bar{f}_1''/f_0'' + \bar{f}_3''/f_0'')] \quad (3d)$$

The functions $f_0(\eta), \bar{f}_1(\eta), \bar{f}_2(\eta)$ and $\bar{f}_3(\eta)$ are the terms of different orders in the expansion of f, as defined in Ref. 1.

Figure 1 shows the different forces acting on the wedge. Assuming that the wedge angle and the angle of attack are small the lift and drag forces can be expressed as[2]:

$$L_p = \int_0^l (p_B^* - p_T^*)dx^* \quad (4a)$$

$$L_v = \int_0^l (\tau_T^*\theta_T - \tau_B^*\theta_B)dx^* \quad (4b)$$

$$D_p = \int_0^l (p_T^*\theta_T + p_B^*\theta_B)dx^* \quad (4c)$$

$$D_v = \int_0^l (\tau_T^* + \tau_B^*)dx^* \quad (4d)$$

The subscripts p and v represent the contributions of the pressure and viscous forces and the subscripts B and T refer to the bottom and top surfaces of the wedge respectively. Writing $\theta_T = \beta - \alpha$ and $\theta_B = \beta + \alpha$ and substituting for p^* and τ^*

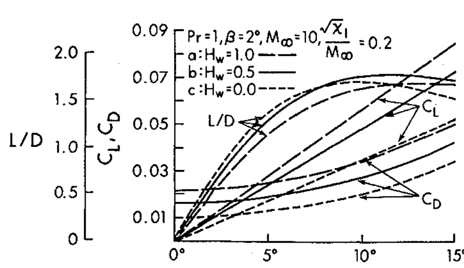

Fig. 2 Effect of changing the surface temperature on the lift coefficient, drag coefficient and lift/drag ratio.

‡ All physical quantities are represented by the superscript * and the subscript ∞ refers to the freestream condition. Quantities, nondimensionalized with respect to the corresponding freestream value, are denoted without any superscript.

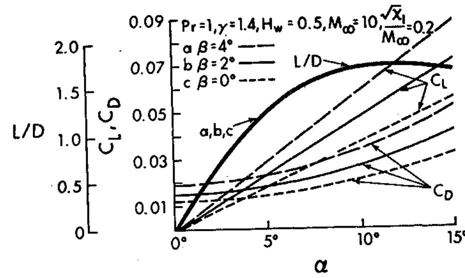

Fig. 3 Effect of changing the semiwedge-angle on the lift coefficient, drag coefficient, and lift/drag ratio.

from the expansions (1) and (2), the Eqs. (4), after the necessary integrations, give

$$C_L = \frac{L_p+L_v}{\rho_\infty^* u_\infty^{*2} l} = 4\alpha\left[\frac{p_0p_3\beta}{\gamma}+\frac{2A}{3}\left\{\frac{p_0p_1}{\gamma}-\frac{\tau_0\tau_2}{M_\infty^2}-\tau_0\tau_3(3\beta^2+\alpha^2)\right\}-2\tau_0\tau_1\beta A^2-2\tau_0A^3\right] \quad (5)$$

$$C_D = \frac{D_p+D_v}{\rho_\infty^* u_\infty^{*2} l} = 2\left[\frac{p_0\beta}{\gamma}\left\{p_3(\beta^2+3\alpha^2)+\frac{p_2}{M_\infty^2}\right\}+\frac{4}{3}A\left\{(\beta^2+\alpha^2)\left(\frac{p_0p_1}{\gamma}+\tau_0\tau_3\right)+\frac{\tau_0\tau_2}{M_\infty^2}\right\}+2A^2\left(\frac{p_0}{\gamma}+\tau_0\tau_1\right)\beta+4\tau_0A^3\right] \quad (6)$$

where $A = \bar{\chi}_l^{1/2}/M_\infty$, $\bar{\chi}_l$ being the interaction parameters evaluated at the end of the wedge.

Figures 2–5 show some of the results of the present analysis. In Fig. 2 C_L, C_D, and L/D ratio are plotted against the angle of attack α for $H_w = 0.0$, 0.5, and 1.0. Both C_L and C_D increase with increasing H_w, but the L/D ratio decreases. In Fig. 3 the effects of changing the semiwedge angle β are shown. Here again, both C_L and C_D increase with increasing β, however, the L/D ratio remains substantially constant. The effect of changing the parameter A ($= \bar{\chi}_l^{1/2}/M_\infty$) on the L/D ratio of a 2° wedge is shown in Fig. 4. The L/D ratio improved significantly with decreasing values of the parameter A. This agrees with the findings of Mirels and Lewellen.[2]

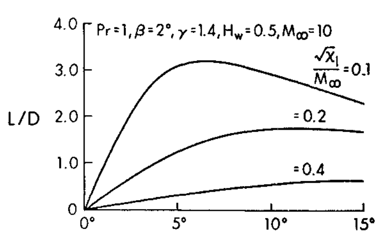

Fig. 4 Effect of changing the parameter A on the lift/drag ratio of a 2° wedge.

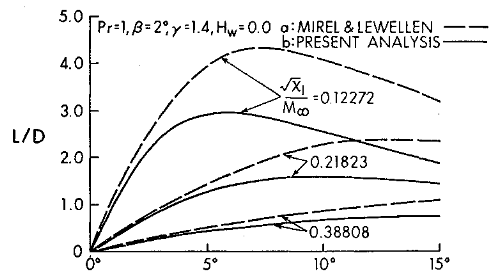

Fig. 5 Effect of changing the parameter A on the lift/drag ratio of a flat plate compared with the results of Ref. 2.

Figure 5 compares the L/D ratio for a flat plate ($\beta = 0$) with the results of Mirels and Lewellen.[2] Agreement is good for small values of the angle of attack.

References

[1] Chattopadhyay, T. K. and Rodkiewicz, C. M., "Hypersonic Strong Interaction Flow Over an Inclined Surface," *AIAA Journal*, Vol. 9, No. 3, 1971, pp. 535–537.

[2] Mirels, H. and Lewellen, W. S., "Hypersonic Viscous Interaction Theory for Wedge Wings," *Journal of Spacecraft and Rockets*, Vol. 4, No. 4, 1967, pp. 492–497.

Structure of Turbulent Diffusion Flames

Paul M. Chung*
University of Illinois, Chicago, Ill.

Nomenclature

C_p = constant pressure specific heat
h = $(C_p/\Delta h^0)t$
Δh^0 = heat of combustion
L = width of the shear or mixing layer
$\hat{M}$ = molecular weight
m = $(d\hat{M}_p/a\hat{M}_r)z_r$
n = $(d\hat{M}_p/b\hat{M}_f)z_f$
t = instantaneous absolute temperature
U_k = $u_k - \langle u_k \rangle$
u_k = absolute velocity vector in tensor notation
u,v,w = x, y, and z components of velocity, respectively
x,y = Cartesian coordinates
x_k = position vector in tensor notation
Y = y/L
z = Cartesian coordinate, or the instantaneous mass fraction
λ = integral scale in the limit of small mean velocity gradient
ρ = density
$\langle Q \rangle$ = $\int fQd\mathbf{U}$

Introduction

In the existing theories wherein the turbulent transport is described phenomenologically as a function of the local properties in analogous to the laminar transport, the mixing of the two fluid elements containing two different chemical reactants will immediately allow the reaction to commence between the two reactants. Therefore, these turbulent mixing theories predict the existence of an infinitesimally thin diffusion flame sheet in the chemically equilibrium limit, as it is with the laminar diffusion flame. A typical analysis leading to such a flame sheet was given by Libby.[1] A chemical reaction, however, is a molecular process, and the mixing of the fluid elements is not sufficient for the combustion of the initially unmixed reactants.

The molecular diffusion of chemical species between the fluid elements which have been mixed takes finite amounts of time and, therefore, the combustion zone must be of finite thickness even in the limit of an infinitely large Damkohler number.

The existing experimental results[2–4] of turbulent diffusion flames bear out the aforementioned aspect of the combustion. The mean concentration profiles of the reactants show that the flame zone wherein both reactants coexist is very thick indeed.

In order to rectify the aforementioned difficulties with the conventional phenomenological theories in describing the mixing and chemical reaction, a simplified statistical theory[5,6] has been developed by the present author for the high turbulence-Reynolds number flows. This theory has been successfully employed to analyze the turbulent flowfield with a uniform mean velocity gradient,[5] which we define as the homologous flowfield. In the present paper, this theory is employed to analyze the structure of the diffusion flame established within an homologous turbulent shear field. The homologous field is chosen because it is the simplest shear field for analysis, and because it is expected that the basic structure of the flame is independent of the flow configuration and boundary conditions as it is with the laminar flames.[7] The details of the results and analyses to be discussed here are found in the AIAA preprint.[8]

Analysis

We consider the mixing layer formed between the two isotropic streams of equal turbulence energy E shown in Fig. 3 of Ref. 5. In order that the flow be homologous, we assume that the mixing layer is bound by two slippery planes, respectively at $Y = 0$ and $Y = 1$, which are perfectly pervious to mass and momentum. We further consider that the stream at $Y = 0$ consists of a pure fuel whereas the stream at $Y = 1$ consists of an oxidant and a chemically inert gas. The two streams are considered to be at the uniform temperatures of $t_1(0)$ and $t_2(1)$, respectively.

We consider that the mean fluctuations of all scalar quantities are zero in the bounding streams. The fluctuations of the scalar quantities in the mixing layer are then caused by the mixing of the chemical species and by the chemical reaction taking place in the layer.

The following one step chemical reaction is considered for the combustion:

$$a(\text{fuel}) + b(\text{oxidant}) \xrightarrow{k} d(\text{product})$$

where a, b, and d denote the number of moles.

The specific rate coefficient k is considered to be given by

$$k = k_o \exp[-\Delta E/(Rt)] \tag{1}$$

where k_o is a constant and ΔE and R are the activation energy and the gas constant, respectively.

The instantaneous rate of generation of the combustion product, W_p, is then given by the law of mass action[7] as

$$W_p = K[\exp - (\Delta E/R)(1/t - 1/t^*)]z_r{}^a z_f{}^b \tag{2}$$

where

$$K = k_o(d\hat{M}_p/\hat{M}_r{}^a\hat{M}_f{}^b)\rho^{a+b-1} \exp - \Delta E/(Rt^*) \tag{3}$$

In the preceding equations, $(\ )^*$ represents the mean chemical equilibrium value at one of the flame edges to be discussed subsequently. The subscripts r, f, c, and p denote the fuel, oxidant, inert gas, and the product, respectively. Note that the meanings of r and f were interchanged in Ref. 8 by mistake.

The instantaneous rates of generation of the fuel, W_r, the oxidant, W_f, and the temperature, W_t, by chemical reaction can be readily related to that of the combustion product.[7]

The starting point of the analysis is the Fokker-Planck equations developed earlier[5] for the flow and scalar fields with no laminar sublayers and mean pressure gradients

$$u_j \frac{\partial f}{\partial x_j} = \frac{\langle U_k U_k \rangle^{1/2}}{2\lambda}\left(1 + \frac{L}{\langle u \rangle_\infty}\frac{\partial \langle u \rangle}{\partial y}\right) \times \left[2\frac{\partial}{\partial U_j}(fU_j) + \frac{\langle U_k U_k \rangle}{3}\frac{\partial^2 f}{\partial U_j \partial U_j}\right] \tag{4}$$

Presented 70-722 at the AIAA Reacting Turbulent Flows Conference, San Diego, Calif., June 17–18, 1970; received August 31, 1970; revision received July 29, 1971. This work is supported by NASA Grant NGR 14-012-012.

Index category: Combustion in Gases.

* Professor of Fluid Mechanics. Member AIAA.